A Lubrication Model of Coating Flows over a Curved Substrate in Space

R. Valéry Roy[*]   A.J. Roberts[†]   M.E. Simpson[‡]

April 23, 1997

Abstract

Consider the three-dimensional flow of a viscous Newtonian fluid upon an abitrarily curved substrate when the fluid film is thin as occurs in many draining, coating and biological flows. We derive a model of the dynamics of the film, the model being expressed in terms of the film thickness and the curvature tensor of the substrate. The model accurately includes the effects of the curvature of the substrate, via a physical multiple-scale approach, and gravity and inertia, via more rigorous centre manifold techniques. Numerical simulations exhibit some generic features of the dynamics of such thin fluid films on substrates with complex curvature.

Contents

[*]Dept of Mechanical Engineering, University of Delaware, USA. E-mail: roy@me.udel.edu

[†]Dept of Mathematics & Computing, University of Southern Queensland, Toowoomba, Queensland 4352, Australia. E-mail: aroberts@usq.edu.au

[‡]Dept of Mathematics & Computing, University of Southern Queensland, Toowoomba, Queensland 4352, Australia. E-mail: simpsonm@usq.edu.au

1   Introduction

The importance of thin-film fluid flows in countless industrial and natural processes has lead to the development of a variety of mathematical models and numerical simulations. This has increased the understanding of the various complex processes at play, such as the effects of generalized Newtonian and shear-thinning rheology of the liquid [37], of geometric complexity of the substrate [29], of multicomponent mixtures and drying processes [4], of surface contamination [30, 31] and roughness [32], of advecting and diffusing contaminants, and of moving substrates. See also for example [6, 16, 17, 18, 28, 35, 38]. Examples of industrial applications include the coating processes of autobodies, beverage containers, sheet goods and films, decorative coating, gravure roll coating, etc. Physical applications can be found in the biomedical field such as the liquid films covering the cornea of the eye or protecting the linings of the lungs [9].

    Herein we consider the slow motion of a thin liquid layer over an arbitrarily curved solid substrate. The fluid is assumed to be incompressible and Newtonian, constituted of a single component and uncontaminated by surface-active material. The substrate is stationary. The effects of substrate curvature on the flow of thin liquid layers driven by surface tension were first modeled by Schwartz & Weidner [29] for two-dimensional geometries. Short-wavelength irregularities of the fluid's free surface are quickly leveled by surface tension forces, but the long-term evolution of the flow is primarily determined by the substrate's curvature. Their calculations confirm qualitative observations of the thinning of coating layers at outside corners and of

the thickening at inside corners. In a subsequent work [30], they studied the joint effect of substrate curvature and the presence of surfactant and showed that corner defects may be significantly altered by the presence of Marangoni forces.

The model derived herein exploits the thinness of the fluid layer and leads to a "lubrication" model of the dynamics whereby the unknown fluid fields are parameterised by only the fluid layer's thickness. Thus, a considerable reduction of the dimensionality of the problem is achieved when compared to the full Navier-Stokes equations. Such thin-geometry or long-wave models have previously been derived in many physical contexts, such as in the mechanics of beams, plates and shells [34, 22], coating flows [13, 27, 3, 1, 35], shallow-water waves [14], viscous fluid sheets [36], etc. On a flat substrate the usual model for the evolution of a viscous film's thickness η, driven only by surface tension, is given by the following non-dimensional equation

$$\frac{\partial \eta}{\partial t} \approx -\tfrac{1}{3} \boldsymbol{\nabla} \cdot \left[\eta^3 \boldsymbol{\nabla} \tilde{\kappa} \right] ,$$

where $\tilde{\kappa} \approx \boldsymbol{\nabla}^2 \eta$ is the curvature of the free surface of the film. Based upon the conservation of fluid and the Navier-Stokes equations, outlined in §§1.1–1.2, we derive in §3 the following model for the evolution of a film on a curved substrate:

$$\frac{\partial \zeta}{\partial t} \approx -\tfrac{1}{3} \boldsymbol{\nabla} \cdot \left[\eta^2 \zeta \boldsymbol{\nabla} \tilde{\kappa} - \tfrac{1}{2} \eta^4 (\kappa \mathbf{I} - \mathbf{K}) \cdot \boldsymbol{\nabla} \kappa \right] , \qquad (1)$$

where $\zeta = \eta - \tfrac{1}{2} \kappa \eta^2 + \tfrac{1}{3} k_1 k_2 \eta^3$ is proportional to the amount of fluid locally above the substrate; $\mathbf{K}$ is the curvature tensor of the substrate; k_1, k_2, and $\kappa = k_1 + k_2$ are the principal curvatures and the mean curvature of the substrate, respectively; and the $\boldsymbol{\nabla}$-operator is expressed in a coordinate system of the substrate, as introduced in §2. This model systematically accounts for the curvature of the substrate and that of the surface of the film. It improves the model derived by Schwartz & Weidner [29] and extends it to flows where the substrate curvature has a larger effect on the fluid dynamics.

Modifications to this model are derived, in §4, when gravity and/or inertia are significant influences. The analysis is performed using computer algebra and is based on centre manifold theory [20] to assure us that all the dynamical effects are incorporated into the model. In centre manifold theory competing small effects need not appear at leading order in the analysis; thus we obtain the flexibility to adapt the model to a variety of parameter regimes *without* redoing the whole analysis. For further discussion of this and other aspects of the application of centre manifold theory to low-dimensional modelling see the review in [26]. Here in particular, the various regimes of gravitational forcing around a curved surface are all encompassed within the one model,

namely equation (50). The terms affected by fluid inertia appear very small in generic situations, see (52), and perhaps may be best used to indicate the error in the lubrication models for moderate Reynolds numbers.

In the last section, §5, we conclude with some numerical simulations of flows on curved surfaces, with attention given to the quantitative differences found between our model and that obtained in [29].

1.1 Equations of motion

We solve the Navier-Stokes equations for an incompressible fluid of density ρ and viscosity μ moving with velocity field $\mathbf{u}$ and pressure field p. The flow is primarily driven by pressure gradients along the substrate and caused by capillary forces characterized by surface tension σ and varying due to variations of the curvature of the free surface of the fluid. However, there may also be a gravitational body force, $\mathbf{g}$, of magnitude g in the direction of the unit vector $\hat{\mathbf{g}}$. Suppose the film has characteristic thickness H. We non-dimensionalise the equations by scaling variables with respect to: the reference length H; the reference time $\mu H/\sigma$; the reference velocity $U = \sigma/\mu$, and the reference pressure σ/H. Thus, in this non-dimensionalisation we take the view of a microscopic creature of a size comparable to the thickness of the fluid; later we require that both the substrate and the free surface curve only gently when viewed on this microscale. The non-dimensional fluid equations are then

$$\boldsymbol{\nabla} \cdot \mathbf{u} \;=\; 0\,, \tag{2}$$

$$\mathcal{R}\left[\frac{\partial \mathbf{u}}{\partial t} + \mathbf{u} \cdot \boldsymbol{\nabla}\mathbf{u}\right] \;=\; -\boldsymbol{\nabla}p + \boldsymbol{\nabla}^2\mathbf{u} + b\hat{\mathbf{g}}\,, \tag{3}$$

where $\mathcal{R} = \sigma\rho H/\mu^2$ is effectively a Reynolds number characterising the importance of the inertial terms—it may be written as UH/ν for the above reference velocity—and $b = \rho g H^2/\sigma$ is a Bond number characterising the importance of the gravitational body force when compared with surface tension.

In §3 we assume that the regime of the flow is characterized by a very small value of the Reynolds number so that the inertia term $\mathcal{R}D\mathbf{u}/Dt$ is neglected in comparison to the viscous forces in the fluid:

$$\mathcal{R} = UH/\nu \ll 1\,.$$

This is the "creeping flow" assumption of lubrication. Later, in §4, we reinstate inertia into the analysis and determine its leading order effects on the dynamics.

1.2 Boundary conditions

Preliminary statements of the boundary conditions are as follows.

1. The fluid immediately in contact with the substrate does not slip along the stationary substrate $\mathcal{S}$, that is

$$\mathbf{u} = \mathbf{0} \quad \text{on } \mathcal{S} \,. \tag{4}$$

2. The kinematic boundary condition at the free surface of the fluid states that fluid particles must follow the free surface.

3. The free surface, denoted by $\mathcal{F}$ and assumed free of contamination, must have zero-shear (tangential stress), namely

$$\tilde{\boldsymbol{\tau}} \cdot \tilde{\mathbf{t}}_1 = \tilde{\boldsymbol{\tau}} \cdot \tilde{\mathbf{t}}_2 = 0 \quad \text{on } \mathcal{F} \,, \tag{5}$$

where $\tilde{\boldsymbol{\tau}}$ is the deviatoric stress acting across $\mathcal{F}$, and $\tilde{\mathbf{t}}_\alpha$ are independent tangent vectors to $\mathcal{F}$. This condition assumes a light and inviscid medium (such as air) above the fluid layer—a condition which guarantees the continuity of the tangential stress as one passes across the interface $\mathcal{F}$.

4. The normal surface stress at $\mathcal{F}$ must account for the surface tension whose effect is to create a discontinuity in the normal stress proportional to the mean curvature of $\mathcal{F}$: in non-dimensional form

$$p = -\tilde{\kappa} + \tilde{\boldsymbol{\tau}} \cdot \tilde{\mathbf{n}} \quad \text{on } \mathcal{F} \,, \tag{6}$$

where p is the fluid pressure relative to the assumed zero pressure of the medium above, and $\tilde{\mathbf{n}}$ is the unit normal to $\mathcal{F}$.

We do not discuss boundary conditions at the lateral extremes of the substrate as the substrate is assumed to be so large in extent, when compared to the fluid thickness, that the dynamics of the fluid film are largely unaffected by the edge boundary conditions. A rational method for deriving boundary conditions for nonlinear dynamical models such as (1) is explained in [21].

2 The adopted coordinate system

The flow is best analysed and solved in a coordinate system that naturally fits the curving substrate. Based upon the principal directions of curvature of the substrate, we construct an orthogonal curvilinear coordinate system in the neighbourhood of the substrate. This natural coordinate system has some remarkable properties which make a systematic analysis tractable.
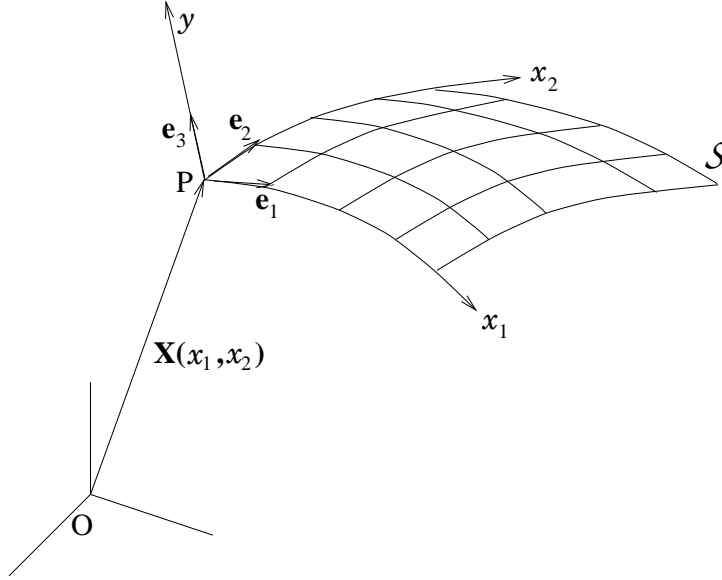
Figure 1: The substrate $\mathcal{S}$ is parameterised by variables x_1 and x_2. Together with the normal distance y, these form an orthogonal curvilinear coordinate system in space with unit vectors $\mathbf{e}_1$, $\mathbf{e}_2$ and $\mathbf{e}_3$.

2.1 The curvilinear coordinate system

The curvilinear coordinate system is taken to be an extension into space of a natural coordinate system of the substrate. We choose, without loss of generality, a curvilinear parameterisation (x_1, x_2) of $\mathcal{S}$ for which the parameter curves $x_1 = \text{Constant}$ and $x_2 = \text{Constant}$ generate the lines of curvature of $\mathcal{S}$ [33], shown schematically in Figure 1. In this case, the curvature tensor becomes diagonal everywhere, with diagonal components k_α.[1]

Conversely, we may view the surface $\mathcal{S}$ as being entirely specified by its metric coefficients $m_\alpha(x_1, x_2)$ and its principal curvatures $k_\alpha(x_1, x_2)$ as functions of the coordinate variables (x_1, x_2) assumed to generate the lines of curvature as the parameter curves of $\mathcal{S}$.

We also define the triad of unit orthogonal vectors $(\mathbf{e}_1, \mathbf{e}_2, \mathbf{e}_3)$ at all points of $\mathcal{S}$: $\mathbf{e}_\alpha$ is tangent to curves of constant $x_{\alpha'}$; and $\mathbf{e}_3$ is normal to $\mathcal{S}$. The metric coefficients, m_α, allow measurement of lengths on $\mathcal{S}$: the arclength of

---

[1]Latin indices (such as i, j) span the numbers $1, 2, 3$ and are attached to spatial quantities, while Greek indices (such as α or β) span the numbers $1, 2$ and are attached to substrate or surface quantities. A dash on Greek indices denotes the complementary value, that is, $\alpha' = 3 - \alpha$. Subscripts following a comma indicate differentiation with respect to the corresponding coordinate. Unless otherwise specified, we do *not* use Einstein's summation convention for repeated indices.

curves on the substrate are found from

$$ds^2 = (m_1 dx_1)^2 + (m_2 dx_2)^2 \,. \tag{7}$$

Note that the unit vectors vary along $\mathcal{S}$ and that their derivatives $\partial \mathbf{e}_i / \partial x_\alpha$ are needed to express the equations of motion and boundary conditions in the curvilinear coordinates.

As shown in Figure 1, the two-dimensional substrate $\mathcal{S}$ is the locus of the endpoints of the position vector $\mathbf{r}_{OP} = \mathbf{X}(x_1, x_2)$, for some domain $\mathcal{D}$ of (x_1, x_2). We prescribe a third coordinate, denoted by either x_3 or y, as the distance measured along the normal $\mathbf{e}_3$ from a given spatial point P to the surface $\mathcal{S}$. Thus the position vector of points P of the fluid may be written as

$$\mathbf{r} = \mathbf{X}(x_1, x_2) + y\mathbf{e}_3(x_1, x_2) \,, \tag{8}$$

where the endpoint of vector $\mathbf{X}$ belongs to the surface $\mathcal{S}$. A large number of important simplifications occur in using this particular orthogonal curvilinear coordinate system, (x_1, x_2, y), that naturally fits the substrate. A definite example for the flow on a torus is given in §§5.3.

We denote by $\eta(t, x_1, x_2)$ the fluid layer's thickness at time t and location (x_1, x_2). The free surface $\mathcal{F}$ of the fluid is thus represented by the equation $y = \eta(t, x_1, x_2)$, and the fluid fills the domain $0 \le y \le \eta(t, x_1, x_2)$. Note that in general, sufficiently far from the substrate for example, the chosen coordinate system does not lead to a one-to-one mapping between coordinate space and physical space. We require that proper conditions between η, k_1 and k_2 are satisfied so that intersections of normals of $\mathcal{S}$ do not occur within the body of the fluid.

The coordinate unit vectors are independent of y and hence are the same unit vectors, $(\mathbf{e}_1, \mathbf{e}_2, \mathbf{e}_3)$, as defined on the substrate but now defined in space neighbouring $\mathcal{S}$. The corresponding *spatial* metric coefficients are

$$h_\alpha = m_\alpha(1 - k_\alpha y) \,, \quad h_3 = 1 \,. \tag{9}$$

By relating the base unit vectors of the rectangular coordinate system to those of the curvilinear coordinate system, see [2, p598] or [19], the spatial derivatives of the curvilinear unit vectors are

$$\mathbf{e}_{i,j} = \frac{\mathbf{e}_i}{h_i} h_{j,i} - \delta_{ij} \sum_{k=1}^{3} \frac{\mathbf{e}_k}{h_k} h_{i,k} \,. \tag{10}$$

However, in the special coordinate system used here, all such expressions simplify to the equivalent expressions on the substrate and independent of y:

$$\mathbf{e}_{\alpha,\alpha} = -\frac{m_{\alpha,\alpha'}}{m_{\alpha'}} \mathbf{e}_{\alpha'} + k_\alpha m_\alpha \mathbf{e}_3 \,, \qquad \mathbf{e}_{\alpha,\alpha'} = \frac{m_{\alpha',\alpha}}{m_\alpha} \mathbf{e}_{\alpha'} \,,$$

$$\mathbf{e}_{3,\alpha} = -k_\alpha m_\alpha \mathbf{e}_\alpha \,, \qquad \mathbf{e}_{i,3} = \mathbf{0} \,. \tag{11}$$

This choice of curvilinear coordinates is needed only for the *derivation* of a reduced-order approximation of the dynamics of coating flows on $\mathcal{S}$. As seen in (1) for example, the model will be ultimately expressed in coordinate-free terms.

2.2 Free-surface geometry

The shape of the free surface is critical in thin film flows: *fluid surface* curvature variations create pressure gradients to drive the fluid flow. To denote a quantity evaluated on the fluid's free surface we generally use an over-tilde (as already done in §§1.2).

The position of points P on the fluid's free surface $\mathcal{F}$ is given by

$$\mathbf{r}_{OP} = \widetilde{\mathbf{X}}(x_1, x_2) = \mathbf{X}(x_1, x_2) + \eta(t, x_1, x_2)\mathbf{e}_3(x_1, x_2). \tag{12}$$

Hence, the surface $\mathcal{F}$ is naturally parameterised by (x_1, x_2), and its tangential vectors, $\tilde{\mathbf{t}}_1$ and $\tilde{\mathbf{t}}_2$, and unit normal vector, $\tilde{\mathbf{n}}$, are given by

$$\tilde{\mathbf{t}}_\alpha = \frac{\partial \widetilde{\mathbf{X}}}{\partial x_\alpha} = \tilde{h}_\alpha \mathbf{e}_\alpha + \eta_{,\alpha} \mathbf{e}_3, \tag{13}$$

$$\tilde{\mathbf{n}} = \frac{\tilde{\mathbf{t}}_1 \times \tilde{\mathbf{t}}_2}{|\tilde{\mathbf{t}}_1 \times \tilde{\mathbf{t}}_2|} \propto -\tilde{h}_2 \eta_{,1} \mathbf{e}_1 - \tilde{h}_1 \eta_{,2} \mathbf{e}_2 + \tilde{h}_1 \tilde{h}_2 \mathbf{e}_3, \tag{14}$$

where $\tilde{h}_\alpha = m_\alpha(1 - k_\alpha \eta)$ are the metric coefficients at the free surface, and where $\eta_{,\alpha} = \partial \eta / \partial x_\alpha$.

At the free surface, $y = \eta$, the kinematic boundary condition must be imposed, namely that fluid particles on the free surface remain on it. This leads to

$$\frac{\partial \eta}{\partial t} = v - \frac{u_1}{\tilde{h}_1}\frac{\partial \eta}{\partial x_1} - \frac{u_2}{\tilde{h}_2}\frac{\partial \eta}{\partial x_2} \quad \text{on } \mathcal{F}. \tag{15}$$

To account for surface tension effects, we need to compute the free surface mean curvature $\tilde{\kappa}$ in terms of the substrate principal curvatures and the film thickness η. A tractable route is to recognise that the effect of surface tension arises through the energy stored in the free surface. Thus its contribution to the dynamical equations, through the curvature $\tilde{\kappa}$, arises from the variation of the surface area with respect to changes in the free-surface shape $y = \eta(t, x_1, x_2)$. The free-surface area is $A = \int dA = \int \mathcal{A}\, dx_1 dx_2$ where

$$\mathcal{A} = \sqrt{\tilde{h}_1^2 \tilde{h}_2^2 + \tilde{h}_2^2 \eta_{,1}^2 + \tilde{h}_1^2 \eta_{,2}^2},$$

is proportional to the free-surface area above a patch $m_1 dx_1 \times m_2 dx_2$ of the substrate. The effect of curvature of the free surface, $\tilde{\kappa}$, is determined from

the variation of $\mathcal{A}$ with respect to η:

$$\tilde{h}_1 \tilde{h}_2 \tilde{\kappa} = -\frac{\delta \mathcal{A}}{\delta \eta} = \frac{\partial}{\partial x_1}\left(\frac{\partial \mathcal{A}}{\partial \eta_{,1}}\right) + \frac{\partial}{\partial x_2}\left(\frac{\partial \mathcal{A}}{\partial \eta_{,2}}\right) - \frac{\partial \mathcal{A}}{\partial \eta} \, .$$

That is,

$$
\begin{aligned}
\tilde{\kappa} \;=\; & \frac{1}{\tilde{h}_1 \tilde{h}_2}\left[\frac{\partial}{\partial x_1}\left(\frac{\tilde{h}_2^2 \eta_{,1}}{\mathcal{A}}\right) + \frac{\partial}{\partial x_2}\left(\frac{\tilde{h}_1^2 \eta_{,2}}{\mathcal{A}}\right)\right] \\
& + \frac{1}{\mathcal{A}}\left[\left(\tilde{h}_1^2 + \eta_{,1}^2\right)\frac{m_2 k_2}{\tilde{h}_1} + \left(\tilde{h}_2^2 + \eta_{,2}^2\right)\frac{m_1 k_1}{\tilde{h}_2}\right] \, .
\end{aligned}
\tag{16}
$$

An approximation is

$$\tilde{\kappa} = \boldsymbol{\nabla}^2 \eta + \frac{k_1}{1 - k_1 \eta} + \frac{k_2}{1 - k_2 \eta} + \mathcal{O}\left(\kappa^3 + \boldsymbol{\nabla}^3 \eta\right) \, ,\tag{17}$$

where it is sufficiently accurate to use the standard form of the Laplacian in the curvilinear coordinates of the substrate,

$$\boldsymbol{\nabla}^2 \eta = \frac{1}{m_1 m_2}\left[\frac{\partial}{\partial x_1}\left(\frac{m_2}{m_1}\frac{\partial \eta}{\partial x_1}\right) + \frac{\partial}{\partial x_2}\left(\frac{m_1}{m_2}\frac{\partial \eta}{\partial x_2}\right)\right] \, .$$

The approximation (17) arises directly from the form of the variational expression and accounts for changes in the free-surface curvature due to the finite depth of the film, and variations in the film thickness.

Note that throughout this paper, $\boldsymbol{\nabla}$ has two different meanings depending upon the context of whether it is applied to three-dimensional spatial fields, such as $\mathbf{u}$ and p, or to two-dimensional substrate fields such as η and κ.

3 Lubrication model driven by surface tension

We now derive a model for the flow dynamics when the fluid film and the substrate vary on a large scale relative to the thickness of the film: because of the two vastly different space scales it may be viewed as a multiple-scale analysis. In this case, viscous dissipation acts quickly across the fluid to damp out all except the slow dynamics associated with such large scale motion. With the assumptions that inertia and body forces can be neglected, by considering conservation of mass we derive an equation for the *slow* evolution of the film thickness η.

3.1   Re-scale the problem

We need to re-scale the non-dimensional governing equations. There are two characteristic lengths of the problem: a reference length L measured along the substrate and a reference thickness H of the fluid layer covering $\mathcal{S}$. The length-scale L is thought of as either the scale of the radius of curvature of the substrate, or as the scale on which the film thickness varies. We generally expect both to be of the same order of magnitude as they both are inversely proportional to substrate gradients, $\boldsymbol{\nabla}\mathbf{n}$ and $\boldsymbol{\nabla}\eta$ respectively. We denote the ratio H/L by ϵ, and assume $\epsilon \ll 1$ to be consistent with the thin-film/large-substrate assumption. In particular, we consider the flow to be non-dimensionally of thickness 1, and so the substrate scale is non-dimensionally of large size $1/\epsilon$.

With the above in mind, we introduce the scaled curvatures (temporarily indicated by a "*" superscript)

$$k_\alpha = \epsilon k_\alpha^*, \quad \text{and } \tilde{\kappa} = \epsilon\tilde{\kappa}^*, \tag{18}$$

to express that the substrate and free-surface curvatures are $\mathcal{O}\left(\epsilon\right)$. Then we scale substrate coordinates and metric coefficients according to

$$m_\alpha = \frac{1}{\epsilon}m_\alpha^*, \quad x_\alpha^* = x_\alpha. \tag{19}$$

This form is appropriate if the substrate coordinates are naturally non-dimensional, such as the angular latitude and longitude coordinates on a sphere. (If you consider the substrate coordinates as naturally lengths, then the alternative scaling $m_\alpha = m_\alpha^*$, $x_\alpha^* = \epsilon x_\alpha$ is appropriate; in this case you would consider x_α^* as a slow-space scale.) The re-scaled spatial metric coefficients then become

$$h_\alpha^* = m_\alpha^*(1 - \epsilon k_\alpha^* y). \tag{20}$$

Seeking a slow flow leads to the following re-scaling of the nondimensional variables for pressure, velocity, and stress:

$$p = \epsilon p^*, \quad u_\alpha = \epsilon^2 u_\alpha^*, \quad v = \epsilon^3 v^*, \quad \boldsymbol{\tau} = \epsilon^2 \boldsymbol{\tau}^*. \tag{21}$$

Now we write the equations and boundary condition in the scaled variables. In what follows, we drop the "*" superscript on all re-scaled variables. First, the continuity equation, $\boldsymbol{\nabla} \cdot \mathbf{u} = \mathbf{0}$,

$$\frac{\partial}{\partial x_1}(h_2 u_1) + \frac{\partial}{\partial x_2}(h_1 u_2) + \frac{\partial}{\partial y}(h_1 h_2 v) = 0, \tag{22}$$

then, the Stokes momentum equation, $\boldsymbol{\nabla} p = \boldsymbol{\nabla}^2 \mathbf{u}$:

$$\frac{\mathbf{e}_1}{h_1}\frac{\partial p}{\partial x_1} + \frac{\mathbf{e}_2}{h_2}\frac{\partial p}{\partial x_2} + \frac{1}{\epsilon}\mathbf{e}_3\frac{\partial p}{\partial y} = \frac{1}{h_1 h_2}\left\{ \epsilon^2\frac{\partial}{\partial x_1}\left(\frac{h_2}{h_1}\frac{\partial}{\partial x_1}\right) + \right.$$

$$\left. +\epsilon^2\frac{\partial}{\partial x_2}\left(\frac{h_1}{h_2}\frac{\partial}{\partial x_2}\right) + \frac{\partial}{\partial y}\left(h_1 h_2\frac{\partial}{\partial y}\right)\right\}(u_1\mathbf{e}_1 + u_2\mathbf{e}_2 + \epsilon v\mathbf{e}_3)\,. \quad (23)$$

The boundary conditions now take the following forms.

- First, the no-slip boundary condition (4) is

$$u_i = 0\,, \quad \text{on } y = 0\,. \tag{24}$$

- Now consider the zero-shear-stress boundary condition at $y = \eta$. First, from (14), express the components of the normal unit vector $\tilde{\mathbf{n}}$ in terms of the scaled variables:

$$c\tilde{n}_\alpha = -\epsilon(1 - \epsilon\eta k_{\alpha'})\frac{\eta_{,\alpha}}{m_\alpha}\,, \quad c\tilde{n}_3 = (1 - \epsilon\eta k_1)(1 - \epsilon\eta k_2)\,, \tag{25}$$

where $c = |\tilde{\mathbf{t}}_1 \times \tilde{\mathbf{t}}_2|$ is the constant of normalisation. Furthermore, from [2, p599], the components of the non-dimensional (symmetric) deviatoric stress tensor, $\boldsymbol{\tau} = (\boldsymbol{\nabla}\mathbf{u} + \boldsymbol{\nabla}\mathbf{u}^T)$, become, upon scaling:

$$\tau_{\alpha\alpha} = 2\epsilon\left[\frac{1}{m_\alpha}\frac{\partial u_\alpha}{\partial x_\alpha} + \frac{m_{\alpha,\alpha'}}{m_1 m_2}u_{\alpha'}\right] + \mathcal{O}\left(\epsilon^2\right)\,,$$

$$\tau_{12} = \epsilon\left[\frac{1}{m_2}\frac{\partial u_1}{\partial x_2} + \frac{1}{m_1}\frac{\partial u_2}{\partial x_1} - \frac{m_{1,2}}{m_1 m_2}u_1 - \frac{m_{2,1}}{m_1 m_2}u_2\right] + \mathcal{O}\left(\epsilon^2\right)\,,$$

$$\tau_{\alpha 3} = \frac{\partial u_\alpha}{\partial y} + \epsilon k_\alpha u_\alpha + \mathcal{O}\left(\epsilon^2\right)\,, \tag{26}$$

$$\tau_{33} = 2\epsilon\frac{\partial v}{\partial y}\,.$$

Thus to order ϵ, the only contributing terms in the boundary condition $\tilde{\boldsymbol{\tau}}\cdot\tilde{\mathbf{t}}_\alpha = 0$ is $\tau_{\alpha 3}\tilde{n}_3$, namely

$$\frac{\partial u_\alpha}{\partial y} + \epsilon k_\alpha u_\alpha + \mathcal{O}\left(\epsilon^2\right) = 0\,. \tag{27}$$

- In order to write down the normal stress boundary condition on the free surface, equation (6), we first need to express the free-surface mean curvature $\tilde{\kappa}$ to order ϵ: from (17) the scaled free-surface mean curvature is

$$\tilde{\kappa} = \kappa + \epsilon\kappa_2\eta + \epsilon\boldsymbol{\nabla}^2\eta + \mathcal{O}\left(\epsilon^2\right)\,,$$

where $\kappa = k_1 + k_2$ and $\kappa_2 = k_1^2 + k_2^2$. Next, the normal surface stress component to order ϵ^2 in scaled form is (using summation)

$$-p + \epsilon \tilde{n}_i \tilde{n}_j \tau_{ij} = -p + 2\epsilon^2 \left(\frac{\partial v}{\partial y} - \frac{\eta_{,1}}{m_1} \frac{\partial u_1}{\partial y} - \frac{\eta_{,2}}{m_2} \frac{\partial u_2}{\partial y} \right) + \mathcal{O}\left(\epsilon^3 \right) .$$

Hence we now write (6) as

$$p = -\kappa - \epsilon \kappa_2 \eta - \epsilon \boldsymbol{\nabla}^2 \eta + \mathcal{O}\left(\epsilon^2 \right) , \quad \text{on } y = \eta ; \tag{28}$$

viscous stresses have no influence on the normal stress to this order in this scaling.

3.2   Perturbation solution

We now find a solution of these equations by assuming a perturbation expansion of the unknown fields in terms of the small parameter ϵ. We write each component in the following expansion:

$$\begin{aligned}
u_\alpha &= u_\alpha^{(0)} + \epsilon u_\alpha^{(1)} + \epsilon^2 u_\alpha^{(2)} + \cdots , \\
v &= v^{(0)} + \epsilon v^{(1)} + \epsilon^2 v^{(2)} + \cdots , \\
p &= p^{(0)} + \epsilon p^{(1)} + \epsilon^2 p^{(2)} + \cdots .
\end{aligned} \tag{29}$$

Then, at the leading order, we find the following equations governing $u_\alpha^{(0)}$, $v^{(0)}$ and $p^{(0)}$:

$$\frac{\partial p^{(0)}}{\partial y} = 0 ,$$

$$\frac{\partial^2 u_\alpha^{(0)}}{\partial y^2} = \frac{1}{m_\alpha} \frac{\partial p^{(0)}}{\partial x_\alpha} , \tag{30}$$

$$\frac{\partial}{\partial x_1}(m_2 u_1^{(0)}) + \frac{\partial}{\partial x_2}(m_1 u_2^{(0)}) + m_1 m_2 \frac{\partial v^{(0)}}{\partial y} = 0 ,$$

with the boundary conditions

$$u_\alpha^{(0)} = v^{(0)} = 0 \quad \text{at } y = 0 ,$$

$$\frac{\partial u_\alpha^{(0)}}{\partial y} = 0 \quad \text{at } y = \eta , \tag{31}$$

$$p^{(0)} = -\kappa \quad \text{at } y = \eta .$$

The solution of these equations is readily found to be the expected locally parabolic flow driven by pressure gradients induced by curvature variations:

$$p^{(0)} = -\kappa ,$$

$$u_\alpha^{(0)} = -\frac{1}{m_\alpha} \kappa_{,\alpha} \left(\tfrac{1}{2} y^2 - \eta y \right) , \tag{32}$$

$$v^{(0)} = \boldsymbol{\nabla}^2 \kappa \left(\tfrac{1}{6} y^3 - \tfrac{1}{2} \eta y^2 \right) - \tfrac{1}{2} \boldsymbol{\nabla} \kappa \cdot \boldsymbol{\nabla} \eta \, y^2 .$$

At the next order of perturbation:

$$\frac{\partial p^{(1)}}{\partial y} = 0 ,$$

$$\frac{\partial^2 u_\alpha^{(1)}}{\partial y^2} - \kappa \frac{\partial u_\alpha^{(0)}}{\partial y} = \frac{1}{m_\alpha} \left(\frac{\partial p^{(1)}}{\partial x_\alpha} + k_\alpha y \frac{\partial p^{(0)}}{\partial x_\alpha} \right) , \tag{33}$$

$$\frac{\partial}{\partial x_1} (m_2 u_1^{(1)}) + \frac{\partial}{\partial x_2} (m_1 u_2^{(1)}) + m_1 m_2 \frac{\partial v^{(1)}}{\partial y} = 0 ,$$

with the boundary conditions

$$u_\alpha^{(1)} = v^{(1)} = 0 \quad \text{at } y = 0 ,$$

$$\frac{\partial u_\alpha^{(1)}}{\partial y} = -k_\alpha u_\alpha^{(0)} \quad \text{at } y = \eta , \tag{34}$$

$$p^{(1)} = - \left(\kappa_2 \eta + \boldsymbol{\nabla}^2 \eta \right) \quad \text{at } y = \eta .$$

We find

$$\begin{aligned}
p^{(1)} &= - \left(\kappa_2 \eta + \boldsymbol{\nabla}^2 \eta \right) , \\
u_\alpha^{(1)} &= -\frac{1}{m_\alpha} (\kappa_2 \eta + \boldsymbol{\nabla}^2 \eta)_{,\alpha} \left(\tfrac{1}{2} y^2 - \eta y \right) - \frac{k_\alpha}{6 m_\alpha} \kappa_{,\alpha} y^3 \\
&\quad - \frac{\kappa}{m_\alpha} \kappa_{,\alpha} (\tfrac{1}{6} y^3 - \tfrac{1}{2} \eta y^2 + \tfrac{1}{2} \eta^2 y) ,
\end{aligned} \tag{35}$$

3.3   Conservation of mass

The expressions in the previous subsection show how the velocity and pressure fields respond to free-surface and substrate curvature. Such flow will thin the film in some places and thicken it in others. Conservation of fluid then leads us to an expression for the evolution of the film's thickness η by the driven flow. Initially we work with non-dimensional but unscaled variables and coordinates before returning to scaled quantities.

Consider a small volume above a patch of the substrate extending across the fluid layer from $y = 0$ to $y = \eta$, see Figure 2. It is bounded by the substrate, the instantaneous free surface and the coordinate surfaces x_1, $x_1 +$
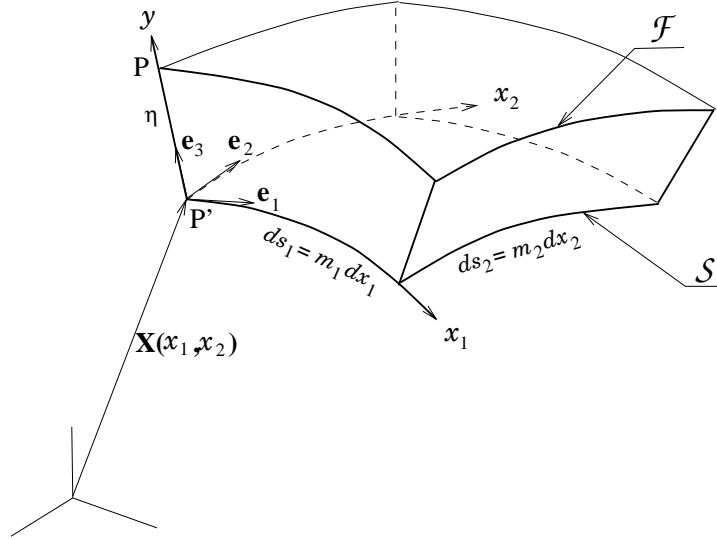
Figure 2: A small control volume V bounded by the substrate, $\mathcal{S}$, the free surface, $\mathcal{F}$, and four coordinate surfaces with separation $m_1 dx_1$ and $m_2 dx_2$.

dx_1, x_2, $x_2 + dx_2$. The rate at which fluid leaves this volume is expressed to first order of infinitesimal quantities dx_1 and dx_2 as the sum of the terms

$$\int_0^{\eta(x_1+dx_1,x_2)} [u_1 h_2 dx_2]_{x_1+dx_1} \, dy - \int_0^{\eta(x_1,x_2)} [u_1 h_2 dx_2]_{x_1} \, dy \,, \qquad (36)$$

for the surfaces x_1 and $x_1 + dx_1$, corresponding terms for the surfaces x_2 and $x_2 + dx_2$, and the term

$$\int_{\mathcal{F}} \mathbf{u} \cdot \tilde{\mathbf{n}} \, dS = \left\{ \tilde{h}_1 \tilde{h}_2 v - \eta_{,1} \tilde{h}_2 u_1 - \eta_{,2} \tilde{h}_1 u_2 \right\} dx_1 dx_2 = \tilde{h}_1 \tilde{h}_2 \frac{\partial \eta}{\partial t} dx_1 dx_2 \,, \quad (37)$$

for the bounding free surface $\mathcal{F}$, where we have used the kinematic boundary condition (15). Upon dividing by $dx_1 dx_2$ and in the limit of $dx_1 dx_2 \to 0$, we deduce

$$m_1 m_2 (1 - \eta k_1)(1 - \eta k_2) \frac{\partial \eta}{\partial t} = -\frac{\partial}{\partial x_1}(m_2 Q_1) - \frac{\partial}{\partial x_2}(m_1 Q_2) \,, \qquad (38)$$

where the Q_α's are the components of the total flux of fluid over a position on the substrate, defined as

$$\mathbf{Q}(t, x_1, x_2) = Q_1 \mathbf{e}_1 + Q_2 \mathbf{e}_2 = \int_0^\eta ((1 - k_2 y) u_1 \mathbf{e}_1 + (1 - k_1 y) u_2 \mathbf{e}_2) dy \,. \quad (39)$$

After division of (38) by $m_1 m_2$, recognize on the right-hand-side the surface divergence of the flux vector $\mathbf{Q}$ expressed in the orthogonal curvilinear coordinate system (x_1, x_2) of $\mathcal{S}$. This yields the divergence form of the conservation

of mass equation:

$$(1-\eta k_1)(1-\eta k_2)\frac{\partial\eta}{\partial t} = -\frac{1}{m_1 m_2}\left(\frac{\partial}{\partial x_1}(m_2 Q_1) + \frac{\partial}{\partial x_2}(m_1 Q_2)\right) = -\boldsymbol{\nabla}\cdot\mathbf{Q}\,. \tag{40}$$

We find an approximation of the flux vector $\mathbf{Q}$ by taking into account the thin layer characteristics of the flow over $\mathcal{S}$ as determined earlier.

Returning to the rescaled quantities introduced in §§3.1, we now determine the perturbation coefficients of the flux vector $\mathbf{Q} = \epsilon^2\mathbf{Q}^{(0)} + \epsilon^3\mathbf{Q}^{(1)} + \cdots$ to be

$$\mathbf{Q}^{(0)} = \int_0^\eta (u_1^{(0)}\mathbf{e}_1 + u_2^{(0)}\mathbf{e}_2)dy = \tfrac{1}{3}\eta^3\left(\frac{\mathbf{e}_1}{m_1}\kappa_{,1} + \frac{\mathbf{e}_2}{m_2}\kappa_{,2}\right) = \tfrac{1}{3}\eta^3\boldsymbol{\nabla}\kappa\,, \tag{41}$$

$$\begin{aligned}
\mathbf{Q}^{(1)} &= \int_0^\eta \left((u_1^{(1)} - k_2 y u_1^{(0)})\mathbf{e}_1 + (u_2^{(1)} - k_1 y u_2^{(0)})\mathbf{e}_2\right)dy \\
&= \tfrac{1}{3}\eta^3\boldsymbol{\nabla}(\kappa_2\eta + \boldsymbol{\nabla}^2\eta) + \tfrac{1}{6}\eta^4\mathbf{K}\cdot\boldsymbol{\nabla}\kappa - \tfrac{1}{3}\eta^4\kappa\boldsymbol{\nabla}\kappa\,,
\end{aligned} \tag{42}$$

where $\kappa = k_1 + k_2$, $\kappa_2 = k_1^2 + k_2^2$, and $\mathbf{K} = k_\alpha\delta_{\alpha\beta}(\mathbf{e}_\alpha : \mathbf{e}_\beta)$ is the curvature tensor (which would not be diagonal in a general orthogonal coordinate system of the substrate $\mathcal{S}$).

Finally, the corresponding evolution equation for η, the so-called lubrication approximation, is given by

$$\begin{aligned}
(1-\epsilon\eta k_1)(1-\epsilon\eta k_2)\frac{\partial\eta}{\partial t} &= -\tfrac{1}{3}\epsilon^3\boldsymbol{\nabla}\cdot\left[\eta^3\boldsymbol{\nabla}\tilde{\kappa} - \epsilon\eta^4\kappa\boldsymbol{\nabla}\kappa + \tfrac{1}{2}\epsilon\eta^4\mathbf{K}\cdot\boldsymbol{\nabla}\kappa\right] \\
&\quad + \mathcal{O}\left(\epsilon^5\right)\,,
\end{aligned} \tag{43}$$

where $\tilde{\kappa} = \kappa + \epsilon\kappa_2\eta + \epsilon\boldsymbol{\nabla}^2\eta + \mathcal{O}(\epsilon^2)$.

We express this equation in the more convenient form

$$\frac{\partial\zeta}{\partial t} = -\tfrac{1}{3}\epsilon^3\boldsymbol{\nabla}\cdot\left[\eta^2\zeta\boldsymbol{\nabla}\tilde{\kappa} - \tfrac{1}{2}\epsilon\eta^4(\kappa\mathbf{I} - \mathbf{K})\cdot\boldsymbol{\nabla}\kappa\right] + \mathcal{O}\left(\epsilon^5\right)\,, \tag{44}$$

where $\zeta = \eta - \tfrac{1}{2}\epsilon\kappa\eta^2 + \tfrac{1}{3}\epsilon^2 k_1 k_2\eta^3$ is proportional to the amount of fluid in the film lying "above" a patch of the substrate. Rewriting this in terms of unscaled, non-dimensional quantities gives (1) when the free-surface curvature is approximated by an expression such as (17).

4 Centre manifold analysis: Gravity and inertia

The previous analysis is adequate to give a basic model for the dynamics of the film thickness. However, it is not clear how to reasonably modify such an

analysis for generally curved substrates in the presence of more complicating physical effects such as gravity. In this section we turn to the more powerful centre manifold theory to extend the previous model in order to include a gravitational body force and to determine the leading effect of inertia. The systematic nature of the centre manifold approach lends itself well towards computer algebra and hence its results provide a valuable check on the human algebra reported in the previous section. In future work, this approach will lead to the correct modelling of initial conditions and forcing, as has been done for dispersion in pipes and channels [15, e.g.], and perhaps small substrate roughness—see the review in [26] for an introduction. This section also serves as an example of the analysis that may be undertaken if other physical effects are needed in the lubrication model of the dynamics.

4.1   Basis of the centre manifold

Centre manifold theory [5] assures us that the long-term dynamics near a fixed point of a dynamical system may be accurately modelled by a "low-dimensional" system which is based upon the linear picture of the dynamics, see the review [26]. Here the lubrication model (1) is of low-dimension in comparison to that of the incompressible Navier-Stokes equations (2–3). The first task is to establish the linear basis of the centre manifold.

Analogous to the approach developed by Roberts in [23, 24], we retain the small parameter ϵ introduced in §3.1 and scale the curvatures and metric coefficients according to (18–19). By considering ϵ negligible we, in the preliminary *linear analysis*, restrict attention to large-scale flows on a flat substrate. However, we do not explicitly scale the unknown fields, p and $\mathbf{u}$ as in (21), because in this approach their scaling naturally arises from the dynamical equations during the course of the analysis rather than being imposed at the outset—another virtue of this approach. Further, we treat the gravitational forcing as a small effect. By substituting, as in [24], the Bond number $b = \beta^2$, then adjoining the trivial equations

$$\frac{\partial \epsilon}{\partial t} = 0\,, \quad \text{and} \quad \frac{\partial \beta}{\partial t} = 0\,, \tag{45}$$

to the scaled versions of the fluid equations (2–3) and their boundary conditions, we treat all terms involving products of $\mathbf{u}$, ϵ and β as perturbing nonlinear terms (as in the centre manifold analysis of the unfolding of bifurcations [5]).

Such nonlinear terms are discarded in the preliminary linear analysis to

leave linear equations

$$\boldsymbol{\nabla} \cdot \mathbf{u} = 0\,, \quad \text{and} \quad \mathcal{R}\frac{\partial \mathbf{u}}{\partial t} + \boldsymbol{\nabla}p - \boldsymbol{\nabla}^2\mathbf{u} = \mathbf{0}\,, \tag{46}$$

where, since $\epsilon = 0$, in effect these differential operators are the Cartesian operators appropriate to a flat substrate. These equations are to be solved with boundary conditions of $\mathbf{u} = \mathbf{0}$ on $\mathcal{S}$ $(y = 0)$ and

$$\frac{\partial u_\alpha}{\partial y} = p - 2\frac{\partial v}{\partial y} = 0 \quad \text{on } y = \eta\,, \tag{47}$$

and the linearized kinematic condition

$$\frac{\partial \eta}{\partial t} - v = 0\,, \quad \text{on } y = \eta\,.$$

All solutions of these linear equations are composed of the decaying lateral shear modes, $v = p = 0$, $u_\alpha = c_\alpha \sin(\ell\pi y/(2\eta))\exp(\lambda t)$ for odd integers ℓ, together with $\eta = \text{constant}$, $u_\alpha = v = p = 0$. In these modes the decay-rate in time is $\lambda = -\ell^2\pi^2/(4\eta^2\mathcal{R})$, except for the last mentioned mode which, as a consequence of fluid conservation, has a decay-rate $\lambda = 0$. So linearly, and in the absence of any lateral variations on a flat substrate, all the lateral shear modes decay exponentially quickly, on a time-scale of $\mathcal{R}\eta^2$, just leaving a film of constant thickness as the permanent mode. This spectrum, of all eigenvalues being strictly negative except for a few that are zero, is the classic spectrum for the application of centre manifold theory; the Existence Theorem 1 in [5] assures us that the nonlinear effects just perturb the linear picture of the dynamics so that in the long-term all solutions of the full nonlinear system are dominated by the slow dynamics induced by gravity and large-scale lateral variations in the film thickness and curvature. The Relevance Theorem 2 in [5] assures us that these dynamics are exponentially attractive and so form a generic model of the long-term fluid dynamics of the film. With the caveat that strict theory has not yet been extended sufficiently to cover this particular application, the closest being that of Gallay [8] and Haragus [11] (but also see [20]), we apply the centre manifold concepts and techniques to systematically develop a low-dimensional lubrication model of the dynamics of the film.

Having identified the critical mode associated with the zero decay-rate, the subsequent analysis is straightforward. The usual approach is to write the fluid fields $\mathbf{v}(t) = (u_1, u_2, v, p)$, as a function of the critical mode η (effectively equivalent to the "slaving" principle of synergetics [10]). Instead of seeking asymptotic expansions in the "amplitude" of the critical mode [20, 15, 23,

e.g.], we apply an algorithm to find the centre manifold and the evolution thereon which is based directly upon the Approximation Theorem 3 in [5, 25] and its variants, as explained in detail by Roberts in [25]. An outline of the procedure follows.

We seek solutions for the fluid fields as

$$\mathbf{v}(t) = \mathbf{V}(\eta), \quad \text{such that} \quad \frac{\partial \eta}{\partial t} = G(\eta, \mathbf{V}(\eta)), \tag{48}$$

where dependence upon the constant parameters (ϵ, β) is implicit, and where G is the right-hand side of the re-scaled version of the kinematic condition (15). The aim is to find the functional $\mathbf{V}$ such that $\mathbf{v}(t)$ as described by (48) forms actual solutions of the scaled Navier-Stokes equations; this ensures fidelity between the model and the fluid dynamics. Suppose that at some stage in an iteration scheme we have an approximation, $\tilde{\mathbf{V}}$ and $\tilde{G} = G(\eta, \tilde{\mathbf{V}})$, and then seek a correction, $\mathbf{V}'$, so that we obtain a more accurate solution to the governing equations. Substituting

$$\mathbf{v}(t) = \tilde{\mathbf{V}} + \mathbf{V}', \quad \text{such that} \quad \frac{\partial \eta}{\partial t} = \tilde{G}$$

into the scaled Navier-Stokes equations then rearranging, dropping products of corrections, and using a zeroth-order approximation wherever factors multiply corrections, we obtain a system of equations for the corrections which is of the form

$$B\mathbf{V}' = \tilde{\mathbf{R}}, \tag{49}$$

where B is the linear operator seen on the left-hand side of (46–47), and, most importantly, $\tilde{\mathbf{R}}$ is the residual of the scaled Navier-Stokes equations using the current approximation. After solving this equation to find the correction $\mathbf{V}'$, the current approximation $\tilde{\mathbf{V}}$ and $\tilde{G}$ is updated. The iteration is repeated until the residual of the governing equations, $\tilde{\mathbf{R}}$, becomes zero to some order of error, whence the centre manifold model will be accurate to the same order of error (by the Approximation Theorem 3 in [5]).

A computer algebra program[2] was written to perform all the necessary detailed algebra for this physical problem. A very important feature of this iteration scheme is that it is performed until the residuals of the actual governing equations are zero, to some order of error. Thus the correctness of the

---

[2]The computer algebra package REDUCE was used because of its flexible "operator" facility. The source code is publicly available via the URL http://www.sci.usq.edu.au/-~robertsa or by contacting the second listed author. At the time of writing, information about REDUCE was available from Anthony C. Hearn, RAND, Santa Monica, CA 90407-2138, USA. E-mail: reduce@rand.org

results that we present here is based only upon the correct evaluation of the residuals and upon sufficient iterations to drive these to zero. Thus the key to the correctness of the results produced by the computer program is the proper coding of the fluid dynamical equations in the chosen curvilinear coordinate system. Upon obtaining the code, these can be seen in the computed residuals within the iterative loop. Also note that because the thickness of the film is continuously varying in space and time, it is convenient to work with equations in terms of a scaled vertical coordinate $Y = y/\eta(\mathbf{x}, t)$ so that the free surface of the film is always $Y = 1$. We also let $X_\alpha = x_\alpha$, $T = t$ complete the new coordinate system. Then space and time derivatives transform according to

$$\frac{\partial}{\partial y} = \frac{1}{\eta}\frac{\partial}{\partial Y}\,, \quad \frac{\partial}{\partial x_\alpha} = \frac{\partial}{\partial X_\alpha} - \frac{Y}{\eta}\frac{\partial\eta}{\partial X_\alpha}\frac{\partial}{\partial Y}\,, \quad \frac{\partial}{\partial t} = \frac{\partial}{\partial T} - \frac{Y}{\eta}\frac{\partial\eta}{\partial T}\frac{\partial}{\partial Y}\,.$$

However, the fluid equations are not rewritten in this new coordinate system because the computer handles all the necessary details of the transformation.

4.2   The general lubrication model

Based upon scalings introduced in §3.1, we run the REDUCE computer algebra program that computes velocity and pressure fields for the flow and the evolution equation for the film's thickness. We find that the evolution equation may be written in the coordinate-free form[3]

$$
\begin{aligned}
\frac{\partial\zeta}{\partial t} \;=\;& -\tfrac{1}{3}\epsilon^3\boldsymbol{\nabla}\cdot\left[\eta^2\zeta\boldsymbol{\nabla}\tilde{\kappa} - \tfrac{1}{2}\epsilon\eta^4(\kappa\mathbf{I} - \mathbf{K})\cdot\boldsymbol{\nabla}\kappa\right] \\
& -\tfrac{1}{3}\epsilon b\boldsymbol{\nabla}\cdot\left[\eta^3\hat{\mathbf{g}}_s - \epsilon\eta^4(\kappa\mathbf{I} + \tfrac{1}{2}\mathbf{K})\cdot\hat{\mathbf{g}}_s + \epsilon\hat{g}_y\eta^3\boldsymbol{\nabla}\eta\right] \\
& +\mathcal{O}\left(\epsilon^5 + b^2\right),
\end{aligned}
\tag{50}
$$

where $\hat{\mathbf{g}}_s$ and $\hat{g}_y$ are respectively the components of the gravitational unit vector tangent and normal to the substrate. Note that in the special orthogonal curvilinear system used in the derivation of the model,

$$\kappa\mathbf{I} - \mathbf{K} = \begin{bmatrix} k_2 & 0 \\ 0 & k_1 \end{bmatrix}, \quad \text{and} \quad \kappa\mathbf{I} + \tfrac{1}{2}\mathbf{K} = \begin{bmatrix} \tfrac{3}{2}k_1 + k_2 & 0 \\ 0 & k_1 + \tfrac{3}{2}k_2 \end{bmatrix}.$$

One example of the application of the model (50) is to the dynamics of thin films on vertical cylinders or fibres as explored by Kalliadasis & Chang

---

[3] $\mathcal{O}\left(\epsilon^p + b^q\right)$ is used to denote terms, z, for which $z/(\epsilon^p + b^q)$ is bounded as $(\epsilon, b) \to \mathbf{0}$. The upshot is that $z = \epsilon^m b^n$ is $\mathcal{O}\left(\epsilon^p + b^q\right)$ iff $m/p + n/q \geq 1$. For example, an expression accurate to $\mathcal{O}\left(\epsilon^5 + b^2\right)$ retains all terms of the form $\epsilon^m b^n$ for $2m + 5n < 10$.

[12]. They find that a thin film may form into drops on the fibre, or may saturate into solitary waves depending upon the film thickness. The model they use, derived by Frenkel [7], is approximately the version of (50) specific to axisymmetric flow around a cylinder of radius a, namely

$$\frac{\partial \zeta}{\partial t} + \frac{1}{3}\frac{\partial}{\partial z}\left[g\eta^3\left(1 + \frac{\eta}{a}\right) + \eta^2\zeta\left(\frac{1}{(a+\eta)^2}\frac{\partial \eta}{\partial z} + \frac{\partial^3 \eta}{\partial z^3}\right)\right] = 0\,, \qquad (51)$$

in our nondimensionalisation, where z measures axial distance and here $\zeta = \eta + \eta^2/2a$. The differences between our systematic approach and theirs is that their model, (2) in [12], does not conserve fluid, while our model (51) does and also has some higher order corrections to account better for the curvature of the substrate. Further, (50) specialised to a cylindrical substrate will also descibe any non-axisymmetric dynamics of interest.

Returning to the general model (50), it is derived solely under the assumptions that curvature and free-surface slopes, as measured by ϵ, and the gravitational forcing, measured by the Bond number b, are perturbing influences. The application of centre manifold theory places no restrictions upon their relative magnitudes—we do *not* have to insist on $b \sim \epsilon$ or any other such relation between these two independent parameters. Provided there are no "run away" instabilities, the model is valid over any scaling regime where both parameters are small. In particular, the model is valid as the tangential and normal gravitational forcing vary widely around a curving substrate.

Also note that the model (50) was derived without placing any overt restriction upon the Reynolds number, it was treated as an $\mathcal{O}(1)$ constant. That the model actually turns out to have no Reynolds number dependence just confirms the Stokes flow nature of these lubrication dynamics. Higher-order analysis, as also seen in [24, §4], shows that inertia first appears at $\mathcal{O}(\epsilon^6 + b^3)$ for fluid films. Thus inertia is formally negligible. However, if the Reynolds number is large enough to be significant, then we have determined that the following $\mathcal{O}(\mathcal{R}\epsilon^6 + \mathcal{R}b^3)$ terms should be included in the evolution equation (50):

$$\begin{aligned}
\frac{\partial \zeta}{\partial t} = \; & \cdots \\
& -\frac{\mathcal{R}}{5}\boldsymbol{\nabla}\cdot\left[\frac{2\eta^6}{3}\left(\boldsymbol{\nabla}\eta\cdot\boldsymbol{\nabla}\kappa\right)\boldsymbol{\nabla}\kappa - \frac{\eta^7}{7}\boldsymbol{\nabla}\left(\boldsymbol{\nabla}\kappa\cdot\boldsymbol{\nabla}\kappa\right) + \frac{26\eta^7}{63}(\boldsymbol{\nabla}^2\kappa)\boldsymbol{\nabla}\kappa\right] \\
& -\frac{2\mathcal{R}b}{15}\boldsymbol{\nabla}\cdot\left[\eta^6\left(\hat{\mathbf{g}}_s\cdot\boldsymbol{\nabla}\eta\,\boldsymbol{\nabla}\kappa + \hat{\mathbf{g}}_s\,\boldsymbol{\nabla}\eta\cdot\boldsymbol{\nabla}\kappa\right) - \frac{3\eta^7}{7}\boldsymbol{\nabla}\left(\hat{\mathbf{g}}_s\cdot\boldsymbol{\nabla}\kappa\right)\right. \\
& \left. \qquad\qquad\qquad + \frac{13\eta^7}{21}\hat{\mathbf{g}}_s\boldsymbol{\nabla}^2\kappa + \frac{13\eta^7}{21}\hat{g}_y\kappa\boldsymbol{\nabla}\kappa\right]
\end{aligned}$$

$$-\frac{2\mathcal{R}b^2}{15}\boldsymbol{\nabla}\cdot\left[\eta^6\hat{\mathbf{g}}_s\left(\hat{\mathbf{g}}_s\cdot\boldsymbol{\nabla}\eta\right)+\frac{\eta^7}{21}(13\kappa\mathbf{I}-9\mathbf{K})\cdot\hat{\mathbf{g}}_s\hat{g}_y\right].\qquad(52)$$

Note that for a flat substrate ($k_1 = k_2 = 0$), these Reynolds number correction terms reduce to those derived by Benney [3] and Atherton & Homsy [1]. We suggest that these terms are more likely to be used to estimate the error in the lubrication model (50) when applied to moderate Reynolds number flows. Thus these expressions may be used to indicate when a more sophisticated dynamical model, such as a two-mode model [6, 23], is required in order to resolve the inertial instabilities of fluid films at higher Reynolds numbers. Also recall from the previous subsection that the time-scale of decay of the lateral shear modes is $\mathcal{R}\eta^2$ and so the other criterion for validity of the model is that the time-scales exhibited in a simulation are significantly longer than this.

Of course, an order of magnitude argument will give a global estimate, over space and time, of the influence of inertia. However, one may make a perfectly satisfactory a priori order of magnitude assessment, but if in a simulation an instability grows, then (52) will detect if it grows too large. Thus (52) supplements order of magnitude estimates by giving focussed *local* estimates of the errors in an actual simulation.

5   Example film flows

In this section we use the preceding lubrication models to demonstrate some of the flow effects caused by substrate curvature.

5.1   Qualitative effect of substrate curvature

Equation (44) shows that, to leading order of perturbation, the flow is driven by substrate curvature gradients, curvature caused by film thickness variations is generally smaller unless the substrate is comparatively gently curved. To understand the effect of curvature qualitatively, consider a two-dimensional flow on a one-dimensional substrate with given curvature κ. Denote $x = x_1$ as substrate arclength so that the scale factor $m_1 = 1$ and there are no variations in x_2. Then to leading order and in the absence of body forces, the flow is governed by the first-order partial differential equation for η:

$$(1-\kappa\eta)\frac{\partial\eta}{\partial t} = -\tfrac{1}{3}\frac{\partial}{\partial x}(\eta^3\kappa_x).\qquad(53)$$
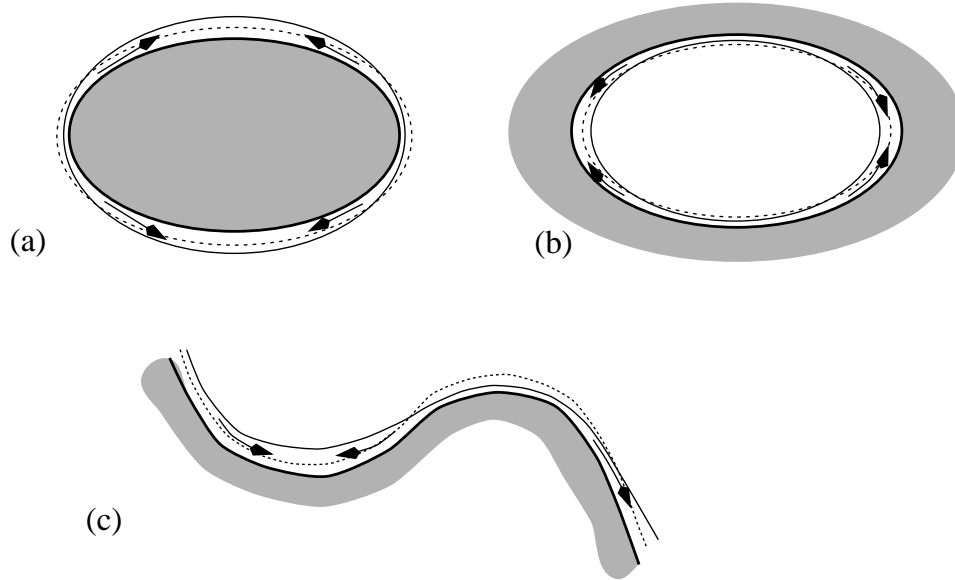
Figure 3: Leading effects of substrate curvature on the evolution of a thin flow

This has a characteristic solution

$$\dot{x} = \kappa_x \frac{\eta^2}{1 - \kappa\eta}, \qquad \dot{\eta} = -\tfrac{1}{3}\kappa_{xx}\frac{\eta^3}{1 - \kappa\eta}. \qquad (54)$$

- Wherever the substrate curvature κ has a local minimum, say at $x = x_0$, then

$$\kappa_x < 0 \ (x < x_0), \quad \kappa_x > 0 \ (x > x_0), \quad \text{and} \quad \kappa_{xx} > 0.$$

   Thus according to the characteristic equations the flow is thinned in the neighborhood of $x = x_0$. Indeed, since $\dot{\eta} \propto -\kappa_{xx}\eta^3$, the film thickness η typically decreases as $t^{-1/2}$ at a point of minimum curvature ($\kappa_{xx} > 0$). As shown schematically in Figure 3, this thinning applies in the neighbourhood of minimum absolute curvature for interior coating flows, and of maximum absolute curvature for exterior coating flows.

- Conversely, the film thickens in the neighbourhood of a point of maximum curvature as also shown in Figure 3. The characteristic solution (54) predicts a film thickness that blows up in finite time. The role of higher-order terms in the model equations is to smooth out such singularity.

5.2   Corner flow

Consider here the two-dimensional fluid dynamics examined by Schwartz & Weidner [29] consisting of the flow which thins a film around an outside corner as shown in Figure 4. The fluid is taken to have surface tension $\sigma = 30$dynes/cm, viscosity $\mu = 1$poise, and density $\rho = 1$gm/cm^3. Initially the film is a uniform 0.01cm thick, corresponding to a Reynolds number of $\mathcal{R} = 0.003$, around the corner which has a radius of 0.1cm. As in the previous subsection, the most convenient way to parameterise the one-dimensional substrate is in terms of the arclength x. In this case our dynamical model (1) reduces to

$$\frac{\partial \zeta}{\partial t} = (1 - \kappa \eta)\frac{\partial \eta}{\partial t} = -\tfrac{1}{3}\frac{\partial}{\partial x}\left[\eta^2 \zeta \frac{\partial \tilde{\kappa}}{\partial x}\right] + \mathcal{O}\left(\epsilon^5\right) , \qquad (55)$$

where $\tilde{\kappa} = \kappa + \kappa^2 \eta + \frac{\partial^2 \eta}{\partial x^2}$, and $\kappa = k_1(x)$ is the curvature of the substrate. In contrast, the model of Schwartz & Weidner (the SaW model) is

$$\frac{\partial \eta}{\partial t} = -\tfrac{1}{3}\frac{\partial}{\partial x}\left[\eta^3 \frac{\partial}{\partial x}\left(\kappa + \frac{\partial^2 \eta}{\partial x^2}\right)\right] . \qquad (56)$$

The differences between the models are that ours includes more terms in the curvature. In particular, ours conserves fluid whereas the SaW model does not. Indeed, in the course of the numerical simulations of the film flow shown in Figure 4, the SaW model lost about 2% of the fluid whereas ours lost none to computational error. For thicker films the difference is more marked.

A numerical scheme to simulate a fluid film via these equations is straightforward. We approximated both (55) and (56) by finite differences on a spatial grid with $N = 97$ points and, because the dynamics are stiff, we employed an implicit integration scheme with time step $\Delta t = 0.00115$s. The numerical scheme uses second-order centred differences in space and time but, in the interests of speed, the nonlinear coefficients are only computed from the earlier time. By varying the size of the space-time grid we determined that these parameters give a numerically accurate simulation.

Shown in Figures 5 and 6 are comparisons between the predictions of the SaW model and ours during the simulation of the thinning of the film around the corner. Observe that the SaW model and ours are quantitatively different: the SaW model predicts a more rapid thinning of the film around the corner, and a slower thickening of the film away from the corner. For example, the thickness at $x = 0$ and $t = 3$s for our model is only reached by the SaW model at time $t \approx 300$s. For quantitative accuracy the thin film flows need the extra curvature terms employed in our model (55).
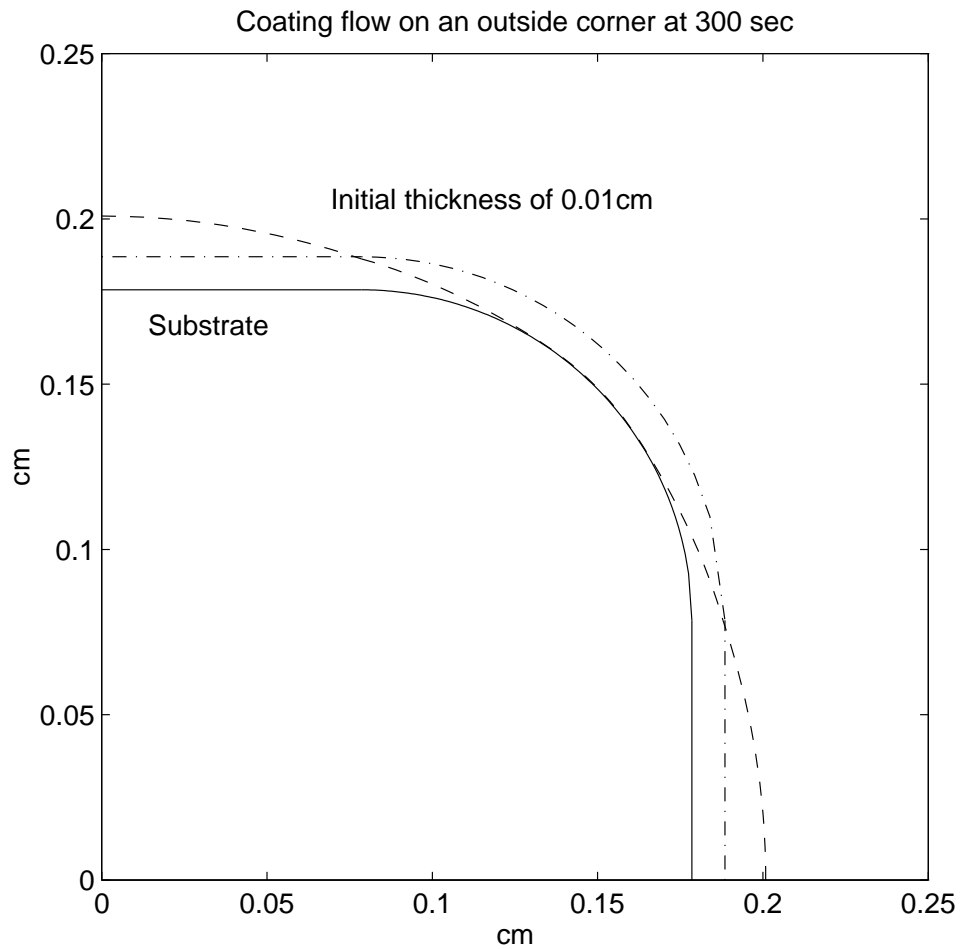
Figure 4: The initial film of fluid (dot-dashed) of constant thickness around a corner (solid) evolves over a long time to thin around the corner (dashed). (Unlike Schwartz & Weidner [29, Fig.7], the thickness of the film has *not* been exaggerated.)
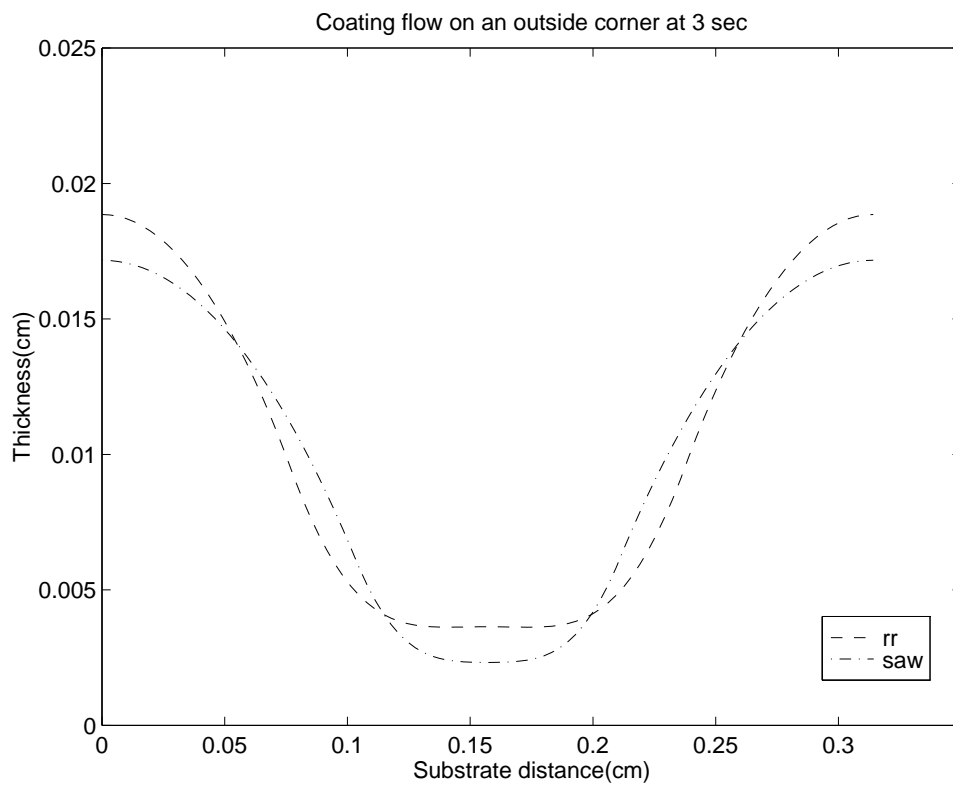
Figure 5: film thickness for the flow around the corner shown in Figure 4 at time $t = 3$s: dashed is our model (55); dot-dashed is the SaW model (56).
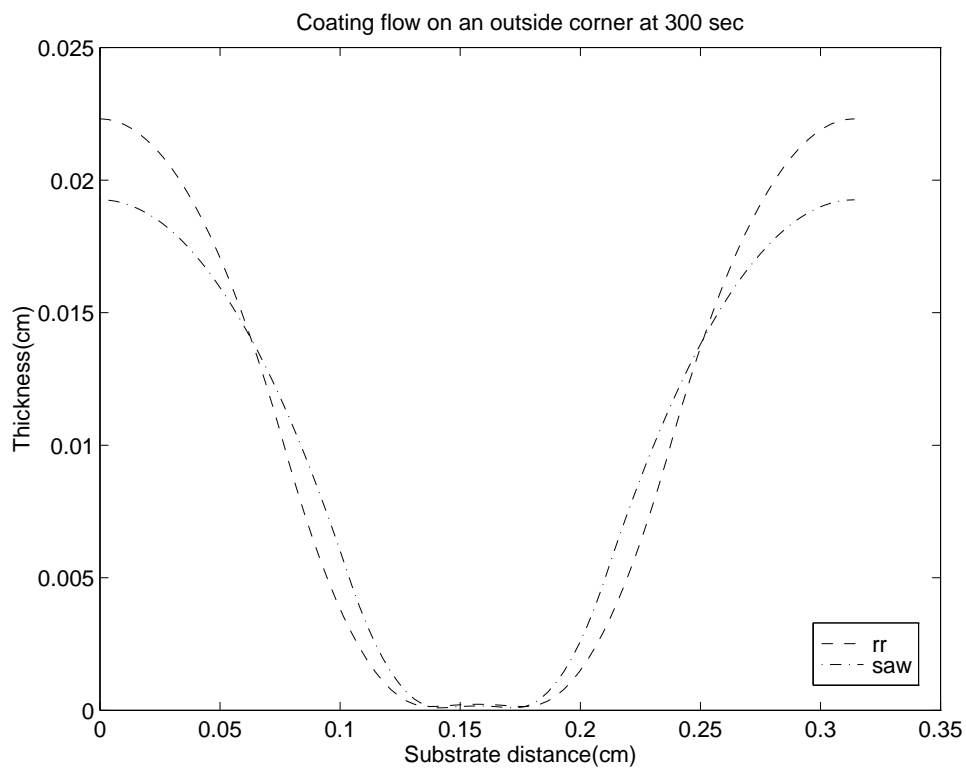
Coating flow on an outside corner at 300 sec

Figure 6: film thickness for the flow around the corner shown in Figure 4 at time $t = 300$s: dashed is our model (55); dot-dashed is the SaW model (56).

Strictly, this corner flow is unsuitable for the lubrication approximation because the sharp change in curvature from the flat wall to the round corner generates arbitrarily large gradients of the curvature κ. These gradients are compounded at higher order. For example, a computation of the Reynolds number terms in the first line of (52) for this problem reveals a relative magnitude, when compared to $\partial \eta / \partial t$, of typically $1000\mathcal{R} \approx 3$. Thus such high-order effects may be significant near the sharp change in curvature. In practise, perhaps we should view the sharp change as an element of roughness in an otherwise smooth transition between the wall and the round corner. Alternatively, we could view it as a discontinuity between two smooth (constant) curvature domains and thereby seek matching conditions via similar arguments to those employed in [21] for boundary conditions.

5.3   Flow around a torus

Here we discuss the evolution of the flow over the surface of a torus with tube of radius R_2 and centreline of radius R_1. We use the following parameterisation:

$$\begin{aligned}
X_1 &= (R_1 + R_2 \cos \theta) \cos \phi \,, \\
X_2 &= (R_1 + R_2 \cos \theta) \sin \phi \,, \\
X_3 &= R_2 \sin \theta \,.
\end{aligned} \tag{57}$$

Take $R_2 < R_1$ to avoid self-intersection, and denote the coordinates $x_1 = \phi$ and $x_2 = \theta$ with $0 \leq \phi < 2\pi$ and $0 \leq \theta < 2\pi$. Then this parameterisation generates an orthogonal curvilinear coordinate system with corresponding orthonormal basis vectors:

$$\begin{aligned}
\mathbf{e}_1 &= \mathbf{e}_\phi = -\sin \phi \mathbf{i} + \cos \phi \mathbf{j} \,, \\
\mathbf{e}_2 &= \mathbf{e}_\theta = -\sin \theta (\cos \phi \mathbf{i} + \sin \phi \mathbf{j}) + \cos \theta \mathbf{k} \,, \\
\mathbf{e}_3 &= \mathbf{e}_1 \times \mathbf{e}_2 = \cos \theta (\cos \phi \mathbf{i} + \sin \phi \mathbf{j}) + \sin \theta \mathbf{k} \,,
\end{aligned} \tag{58}$$

in terms of the unit vectors of the conventional Cartesian coordinate system, and with the corresponding surface metrics

$$m_1 = m_\phi = R_1 + R_2 \cos \theta \,, \quad m_2 = m_\theta = R_2 \,. \tag{59}$$

The chosen coordinate system also generates lines of principal curvature as the parameter curves. We then obtain the following principal curvatures and mean curvature:

$$k_1 = -\frac{\cos \theta}{R_1 + R_2 \cos \theta} \,, \quad k_2 = -\frac{1}{R_2} \,, \quad \kappa = -\frac{1}{R_2} \frac{R_1 + 2R_2 \cos \theta}{R_1 + R_2 \cos \theta} \,. \tag{60}$$

The mean curvature of the substrate is maximum at the inner rim of the torus ($\theta = \pi$), and minimum at the outer rim ($\theta = 0$). Hence we expect the

fluid layer to thicken around the inner rim, and to thin around the outer, solely due to surface tension effects.

We numerically solve the model (44). For simplicity, we seek axisymmetric solutions, that is solutions independent of the angle ϕ around the rim of the torus, and so the film thickness depends only upon θ, the angle around the tube, and t. We try the following form for η

$$\eta(t, \theta) = \sum_{n=0}^{N-1} a_n(t) \cos(n\theta) \,, \tag{61}$$

which guarantees the periodicity of the solution and imposes symmetry across the plane $z = 0$. The ordinary differential equations for the coefficients a_n are found by a Galerkin method where they are determined by making the corresponding residual error orthogonal to the N basis functions, $\cos(n\theta)$, in the usual L_2 norm. As a check, we confirm that the total volume enclosed between the free surface of the fluid and the toroidal substrate remains constant in time. Two numerical simulations were done.

- First, we start with an initially uniform layer of thickness $\eta_0 = 0.1$ on a torus with $R_1 = 2$ and $R_2 = 1$. The corresponding flow towards the inner rim of the torus is shown by the evolution of the film thickness in Figure 7.

- Second, we simulated the flow evolving from a strip of fluid placed around the outer rim of the torus. Again, as shown in Figure 8, the fluid flows around to the inner rim.

On the torus, the importance of inertia effects on this lubrication flow are estimated by the ratio between typical values of the right-hand side of (44) and that of (52): dominantly

$$\text{inertia : lubrication} \approx \frac{\mathcal{R}\eta^4}{6R_1 R_2^2} \,.$$

As may be expected, a thicker film or a more sharply curved torus are more likely to be affected by such higher-order influences. Note that for flows inside a toroidal tube, the thinning of the liquid layer occurs around the inner rim ($\theta = \pi$). Three-dimensional simulations of coating flows exhibiting transversal instabilities (along the ϕ-direction) similar to those found in [39] will be published elsewhere.
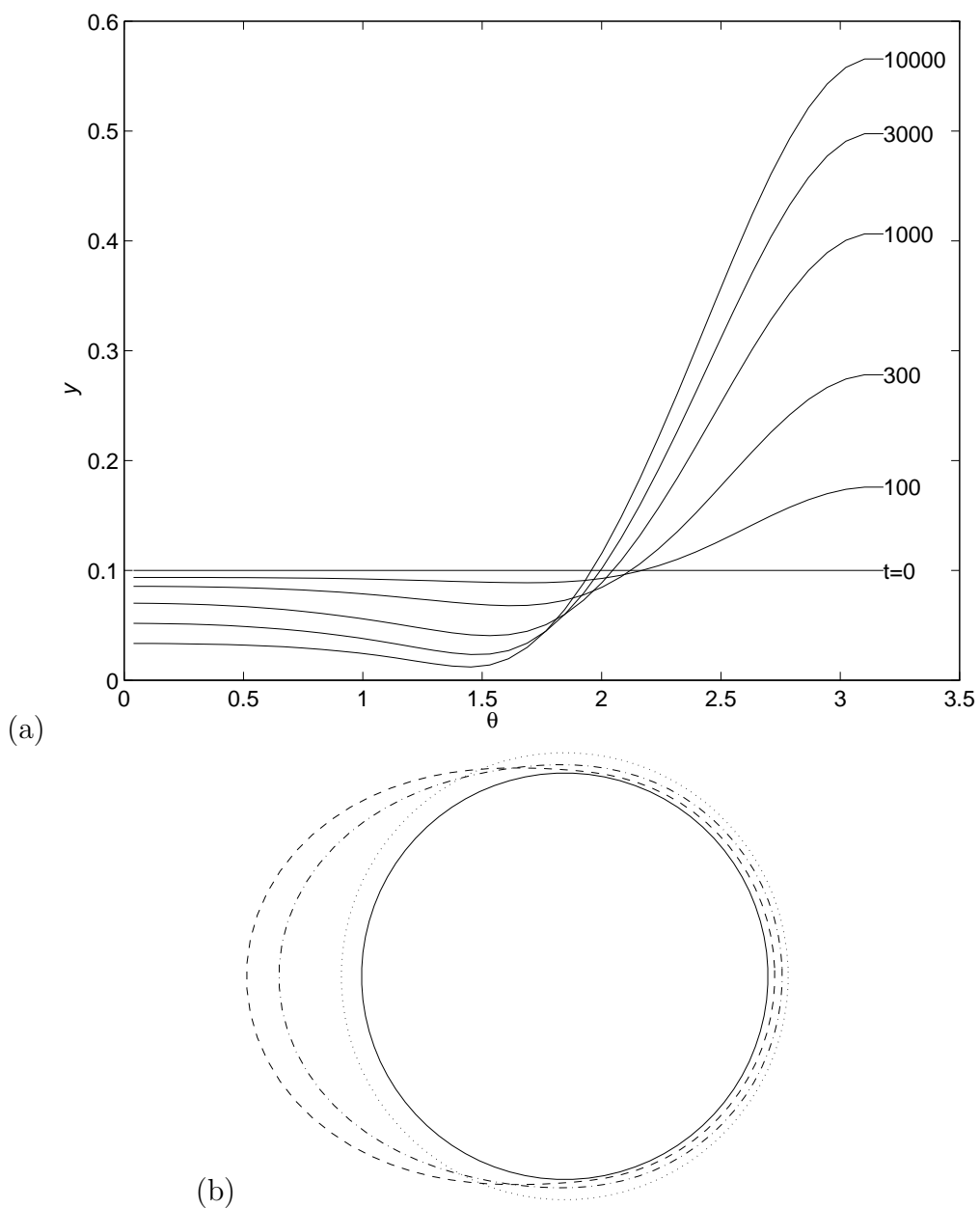
(a)

(b)

Figure 7: evolution of flow on the surface of a torus with $N = 15$ terms in Galerkin approximation. $R_1 = 2$, $R_2 = 1$, $\eta_0 = 0.1$: (a) $\eta(t, \theta)$ shown at $t = 0$, 100, 300, 1000, 3000, 10000; (b) initial, intermediate ($t = 1000$) and late ($t = 10000$) stages of the film on a cross-section of the torus.
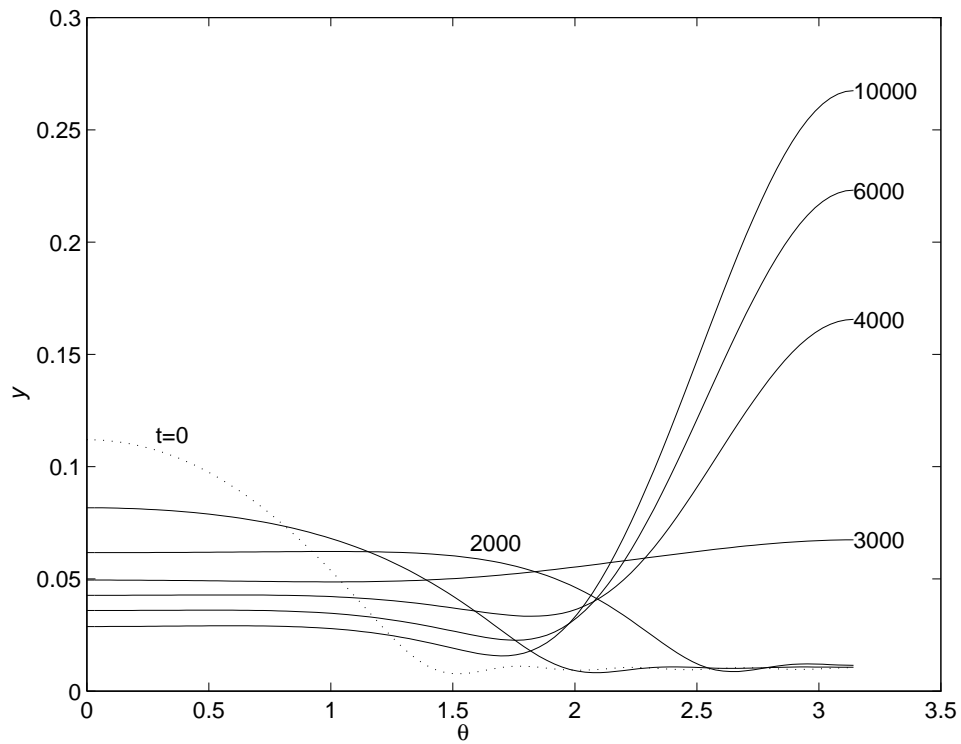
Figure 8: Same as Figure 7 with a step-like initial layer (dotted). $N = 15$ and $t = 0, 1000, 2000, 3000, 4000, 6000, 8000, 10000$.

References

[1] R.W. Atherton and G.M. Homsy. On the derivation of evolution equations for interfacial waves. *Chem. Eng. Comm.*, 2:57–77, 1976.

[2] G.K. Batchelor. *An Introduction to Fluid Dynamics*. CUP, 1979.

[3] D.J. Benney, Long waves on liquid films. J. Math & Physics, 45:150-155, 1966.

[4] R.A. Cairncross, L.F. Francis and L.E. Scriven. *Predicting drying in coatings that react and gel—Drying regime maps*. *AICHE Journal*, 42:55–67, 1996.

[5] J. Carr. *Applications Of Centre Manifold Theory*, volume 35 of *Applied Math Sci.* Springer-Verlag, 1981.

[6] H.C. Chang. Wave evolution on a falling film. *Annu. Rev. Fluid Mech.*, 26:103–136, 1994.

[7] A.L. Frenkel. Nonlinear theory of strongly undulating thin films flowing down vertical cylinders. *Europhys Lett*, 18:583–588, 1992.

[8] Th. Gallay. A center-stable manifold theorem for differential equations in Banach spaces. *Commun. Math. Phys*, 152:249–268, 1993.

[9] J.B. Grotberg. Pulmonary flow and transport phenomena. *Annu. Rev. Fluid Mech.*, 26:529–571, 1994.

[10] H. Haken. *Synergetics, An introduction*. Springer, Berlin, 1983.

[11] M. Hărăguş. Model equations for water waves in the presence of surface tension. *preprint*, 1995.

[12] S. Kalliadasis and H.-C. Chang. Drop formation during coating of vertical fibres. *J Fluid Mech*, 261:135–168, 1994.

[13] V.G. Levich. *Physicochemical Hydrodynamics*. Prentice-Hall, 1962.

[14] C.C. Mei. *The Applied Dynamics of Ocean Surface Waves*, World Scientific, 1989.

[15] G.N. Mercer and A.J. Roberts. A centre manifold description of contaminant dispersion in channels with varying flow properties. *SIAM J. Appl. Math.*, 50:1547–1565, 1990.

[16] J.A. Moriarty, L.W. Schwartz, and E.O. Tuck. Unsteady spreading of thin liquid films with small surface tension. *Phys. Fluids A*, 3:733–742, 1991.

[17] J.A. Moriarty and L.W. Schwartz. Effective slip in numerical calculations of moving-contact line problems. *J. Eng. Math.*, 26:81–86, 1992.

[18] J.A. Moriarty and L.W. Schwartz. Dynamic considerations in the closing and opening of holes in thin liquid films. *J. Colloid Interface Sci.*, 161:335–342, 1993.

[19] P. Morse and H. Feshbach. *Methods of Mathematical Physics*. McGraw-Hill, New York, 1953.

[20] A.J. Roberts. The application of centre manifold theory to the evolution of systems which vary slowly in space. *J. Austral. Math. Soc. B*, 29:480–500, 1988.

[21] A.J. Roberts. Boundary conditions for approximate differential equations. *J. Austral. Math. Soc. B*, 34:54–80, 1992.

[22] A.J. Roberts. The invariant manifold of beam deformations. Part 1: the simple circular rod. *J. Elasticity*, 30:1–54, 1993.

[23] A.J. Roberts. Low-dimensional models of thin film fluid dynamics. *Phys. Letts. A*, 212:63–72, 1996.

[24] A.J. Roberts. An accurate model of thin 2D fluid flows with inertia on curved surfaces. In P.A. Tyvand, editor, *Free-surface flows with viscosity*, Advances in Fluid Mechanics Series. Comput Mech Pub, 1996.

[25] A.J. Roberts. Low-dimensional modelling of dynamics via computer algebra. *Comput Phys Comm*, 100:215–230, 1997.

[26] A.J. Roberts. Low-dimensional modelling of dynamical systems. preprint, USQ, Feb 1997.

[27] G.J. Roskes. Three-dimensional long waves on a liquid film. *Phys. Fluids*, 13:1440–1445, 1969.

[28] K.J. Ruschak. Coating flows. *Annu. Rev. Fluid Mech.*, 17:65–89, 1985.

[29] L.W. Schwartz and D.E. Weidner. Modeling of coating flows on curved surfaces. *J. Engrg. Math.*, 29:91–103, 1995.

[30] L.W. Schwartz, D.E. Weidner, and R.R. Eley. An analysis of the effect of surfactant on the leveling behavior of a thin liquid coating layer. *Langmuir*, 11:3690–3693, 1995.

[31] L.W. Schwartz, R.A. Cairncross and D.E. Weidner. Anomalous behavior during leveling of thin coating layers with surfactants. *Phys. Fluids A*, 8:1693–1695, 1996.

[32] J.B. Sweeney, T. Davis, L.E. Scriven, and J.A. Zasadzinski. Equilibrium thin films on rough surfaces. 1. Capillary and disjoining effects. *Langmuir* 9:1551–1555, 1993.

[33] J.J. Stoker. *Differential geometry*. Wiley-Interscience, New York, 1969.

[34] S.P. Timoshenko and S. Woinowsky-Krieger. *Theory of Shells and Plates*. McGraw Hill, 1959.

[35] E.O. Tuck and L.W. Schwartz. A numerical and asymptotic study of some third-order ordinary differential equations relevant to draining and coating flows. *SIAM Review*, 32:453–469, 1990.

[36] B.W. van de Fliert, P.D. Howell, and J.R. Ockendon. Pressure-driven flow of a thin viscous sheet. *J. Fluid Mech.*, 292:359-376, 1995.

[37] D.E. Weidner and L.W. Schwartz. Contact-line motion of shear-thinning liquids. *Phys. Fluids*, 6:3535-3538, 1994.

[38] D.E. Weidner, L.W. Schwartz and R.R. Eley. Role of surface tension gradients in correcting coating defects in corners. *J. Colloid Interface Sci.*, 179:66-75, 1996.

[39] D.E. Weidner, L.W. Schwartz and M.H. Eres. Simulation of coating layer evolution and drop formation on horizontal cylinders. *J. Colloid Interface Sci.*, 187:243–258, 1997.